Supporting Information

How do copper sites in Cu/H-ZSM-5 zeolites interact with adsorbed alkenes?

Zoya N. Lashchinskaya,[a] *Inga A. Kampf,*[a,b] *Denis D. Mishchenko,*[c] *Svetlana A. Yashnik,*[a] *Andrey A. Saraev,*[c] *Igor. E. Soshnikov,*[a] *Igor P. Prosvirin,*[a] *Anton A. Gabrienko,**[,a] *and Alexander G. Stepanov**[,a]

[a]Boreskov Institute of Catalysis, Siberian Branch of the Russian Academy of Sciences, Prospekt Akademika Lavrentieva 5, Novosibirsk 630090, Russia

[b]Novosibirsk State University, Pirogova Street 2, Novosibirsk, 630090, Russia

[c]Synchrotron Radiation Facility SKIF, Boreskov Institute of Catalysis SB RAS, Kol'tsovo 630559, Russia

* E-mail: gabrienko@catalysis.ru (A.A. Gabrienko)

* E-mail: stepanov@catalysis.ru (A.G. Stepanov)

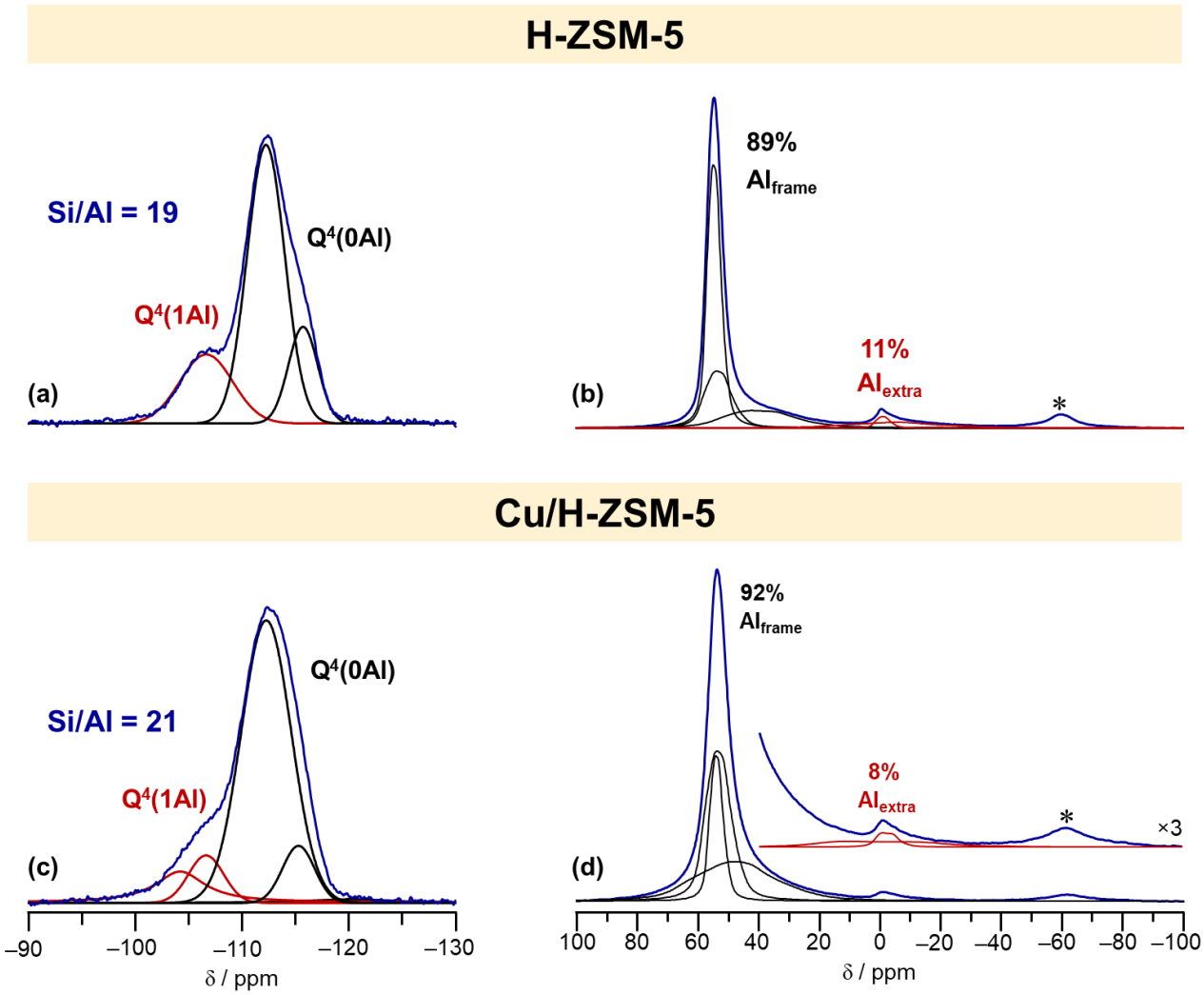

Figure S1. ^{29}Si MAS NMR (a, c) and ^{27}Al MAS NMR (b, d) spectra of the parent H-ZSM-5 sample (a, b) and Cu/H-ZSM-5 sample (c, d). Asterisks (*) denote spinning sidebands.

In ^{29}Si MAS NMR spectra, the signals from different structural units are seen: $Q^4(0Al)$ from $Si(OSi)_4$ fragments and $Q^4(1Al)$ from $Si(OSi)_3(OAl)$ fragments.[1] The spectra were deconvoluted using DMFIT software.[2] The consideration of the relative integrated intensities of the $Q^4(0Al)$ and $Q^4(1Al)$ signals gave the Si/Al framework ratios of 19 and 21 for H-ZSM-5 and Cu/H-ZSM-5 samples, respectively.[1]

In ^{27}Al MAS NMR spectra, the signals from framework AlO_4 units and extra-framework Al species are detected. The spectra were deconvoluted using quadrupole lines and a broadening of Em = 600 with DMFIT software.[2] The parameters of the signals (isotropic chemical shift, quadrupole coupling constant, and asymmetry parameter) are given in Table S1. The spectrum integration revealed the relative content of extra-framework Al to be 11 % and 8 % in H-ZSM-5 and Cu/H-ZSM-5 samples, respectively.

It should be noted that the signals in ^{29}Si and ^{27}Al MAS NMR spectra of Cu/H-ZSM-5 sample are slightly broadened as compared to H-ZSM-5 sample, which is likely the effect of Cu^{2+} paramagnetic sites. The differences in Si/Al ratio and extra-framework Al content determined for H-ZSM-5 and Cu/H-ZSM-5 samples may also be related to the presence of paramagnetic Cu^{2+} sites in Cu/H-ZSM-5 sample.

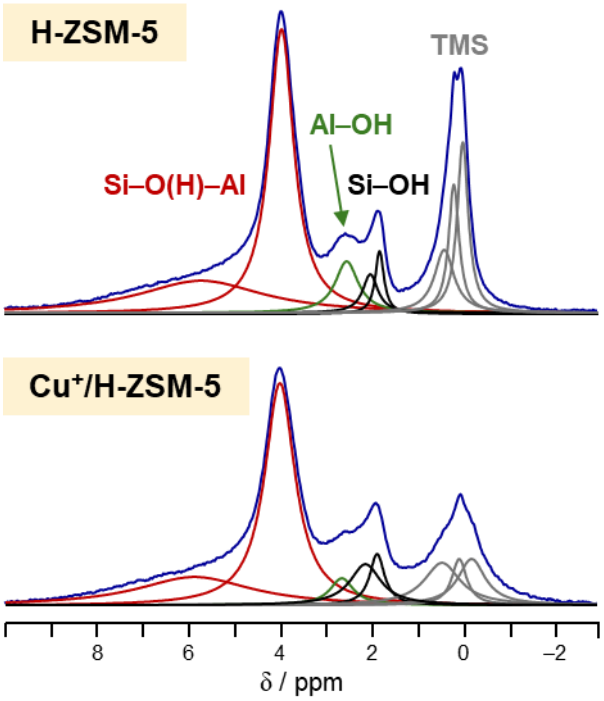

Figure S2. ^{1}H MAS NMR spectra of the parent H-ZSM-5 and Cu^{+}/H-ZSM-5 samples with adsorbed tetramethylsilane (TMS) as an internal standard. The spectra show the signals at 4.0 and 5.9 ppm from isolated and H-bonded Si–O(H)–Al groups, at 2.5–2.6 ppm from Al–OH groups, at 1.8 and 2.0–2.1 ppm from Si–OH groups, and at –0.2–0.4 ppm from TMS. The spectra were deconvoluted using Lorentz lines with DMFIT software.[2] Taking into account the integrated intensities of the signals and the known concentration of TMS, the concentration of Si–O(H)–Al groups was determined for both samples: 950 and 730 μmol g^{-1} for H-ZSM-5 and Cu^{+}/H-ZSM-5 samples, respectively. Note, the accuracy of the method is 5–15 %.[3]

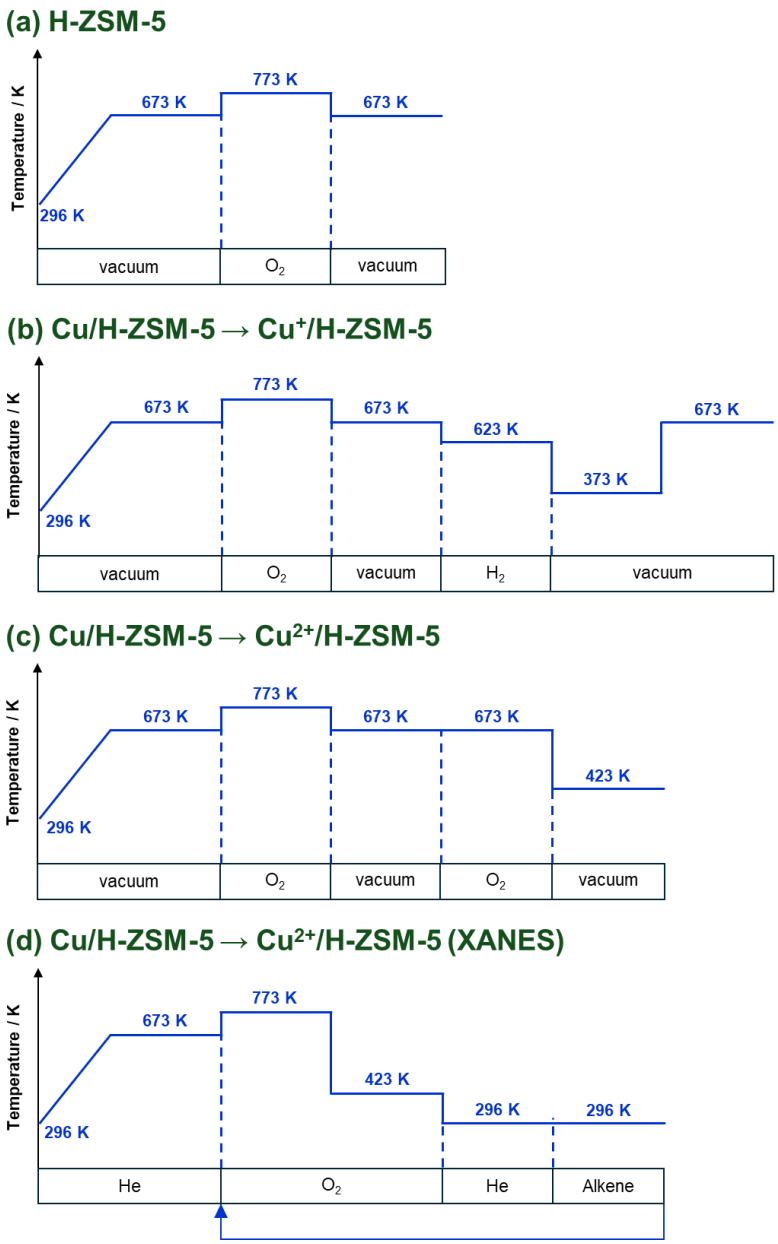

Figure S3. Schematic experimental protocols for zeolite sample activation prior to spectroscopic measurements: schemes (a–c) are relevant for FTIR, NMR, EPR, and XPS studies which involved sample preparation using a vacuum line, while scheme (d) describes XANES experiments which were performed using a flow system. The description of experimental details (the durations of each step, the specific parameters of evacuation and H_2/O_2 treatments) can be found in the Experimental Section.

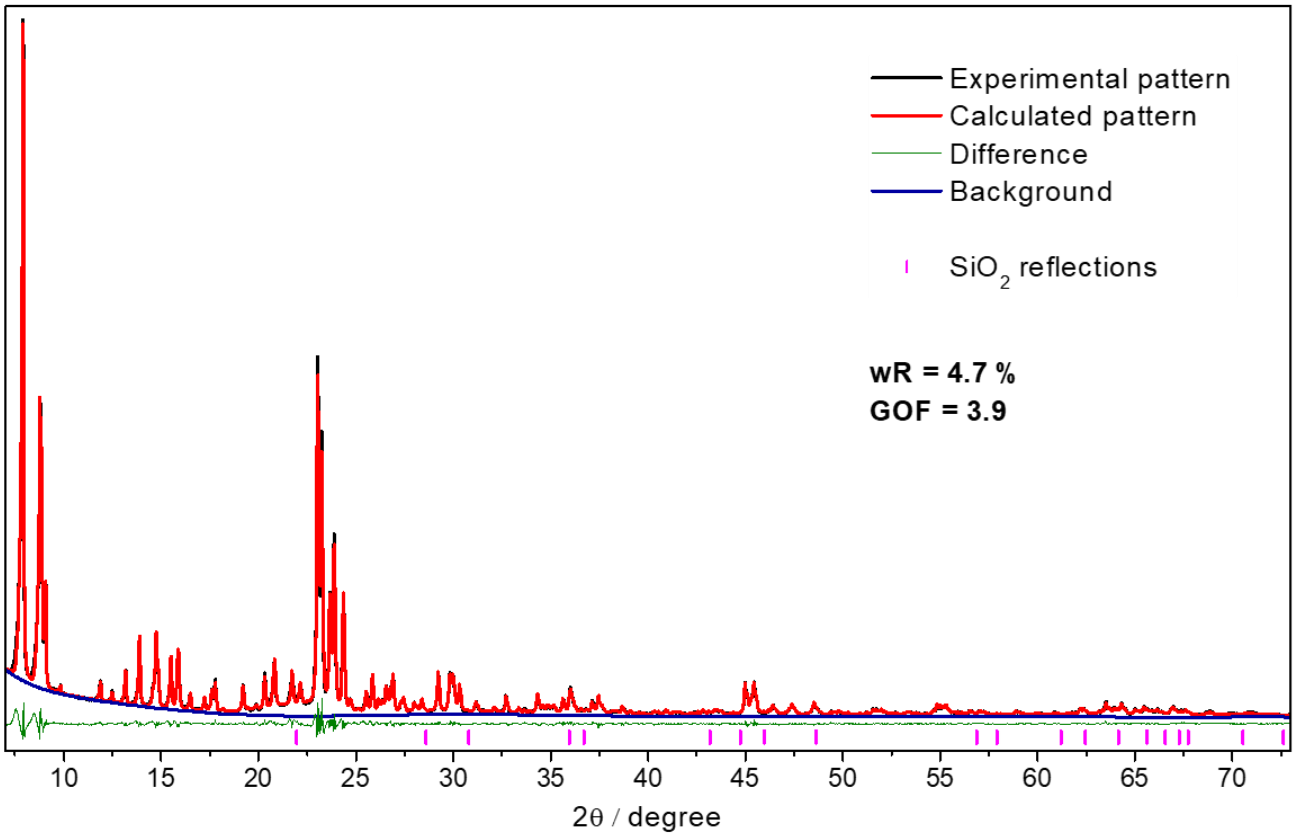

Figure S4. X-ray diffraction pattern of Cu^{2+}/H-ZSM-5 sample (black line) and Rietveld refinement profile (red line). Difference line is shown in green, background is shown in dark blue. Magenta ticks indicate the reflections of SiO_2 admixture. Prior to XRD analysis, the sample was purged with He flow at 673 K, followed by treatment with He:O_2 (1:1) mixture at 773 K (for the detailed procedure, see experimental section, subsection **X-ray diffraction analysis**). The XRD pattern was collected at 296–298 K.

The XRD pattern shows that the sample mainly consists of a phase having an orthorhombic structure (*Pnma* space group) characteristic of ZSM-5 zeolite.[4, 5] Minor admixture phase of SiO_2 in cristobalite modification was also identified (reflections indicated with magenta ticks in Figure S4). Lattice parameters and the size of the coherent scattering region obtained from Rietveld refinement analysis are given in Table S2.

Rietveld refinement of the data was performed to determine the positions of Cu in the zeolite structure. The starting zeolite framework model for the refinement was taken from ref. [6]. Due to the low sensitivity of X-rays to differences in one electron, all twelve T positions of the framework were refined as Si atoms with no Al atoms included. H atoms were also not included in the refinement. This approach required some constraints on the isotropic displacement parameters to keep them within a realistic range. The background function used was a 12-coefficient Chebyshev-1 function constructed from manually specified fixed points. Since the XRD pattern of the zeolite sample shows strong reflections at $2\theta < 10°$, it is necessary to refine Surface roughness B parameter to correctly describe the intensity of such reflections. The impact of this parameter on the quality of the fit can be assessed from Parameter impact function of the GSAS-II software.[7] The refinement results (atom coordinates and isotropic displacement parameters) are presented in Table S3. The best fit is characterized by weighted R-factor (wR) of 4.684 % and the goodness of fit (GOF) of 3.86.

Although, some water molecules were present in the zeolite pores (presumably, due to insufficient dehydration in He flow), Cu cations were found to be coordinated to the framework oxygen atoms and not to the remaining water molecules. The positions of the remaining water molecules and Cu cations were identified by analyzing the difference Fourier maps after refining the zeolite framework structure. During the refinement, the positions of Cu cations were restrained not to be closer than 1.8 Å to the nearest oxygen atom.[8]

Four positions of Cu^{2+} ions in Cu^{2+}/H-ZSM-5 were thus identified as shown in Figure S5. Cu(1) position is located on the wall of the straight channel in a pentasil ring adjacent to an α-site.[9-11] Similar sites were discussed for Cu- and Zn-modified zeolites in refs [9, 12]. Cu(2) position is located

in a four-membered ring on the zigzag channel wall. Cu(3) position lies between two β-sites[9-11] on the zigzag channel wall. Cu(4) position corresponds to a Cu^{2+} ion in the δ-site.[9-11]

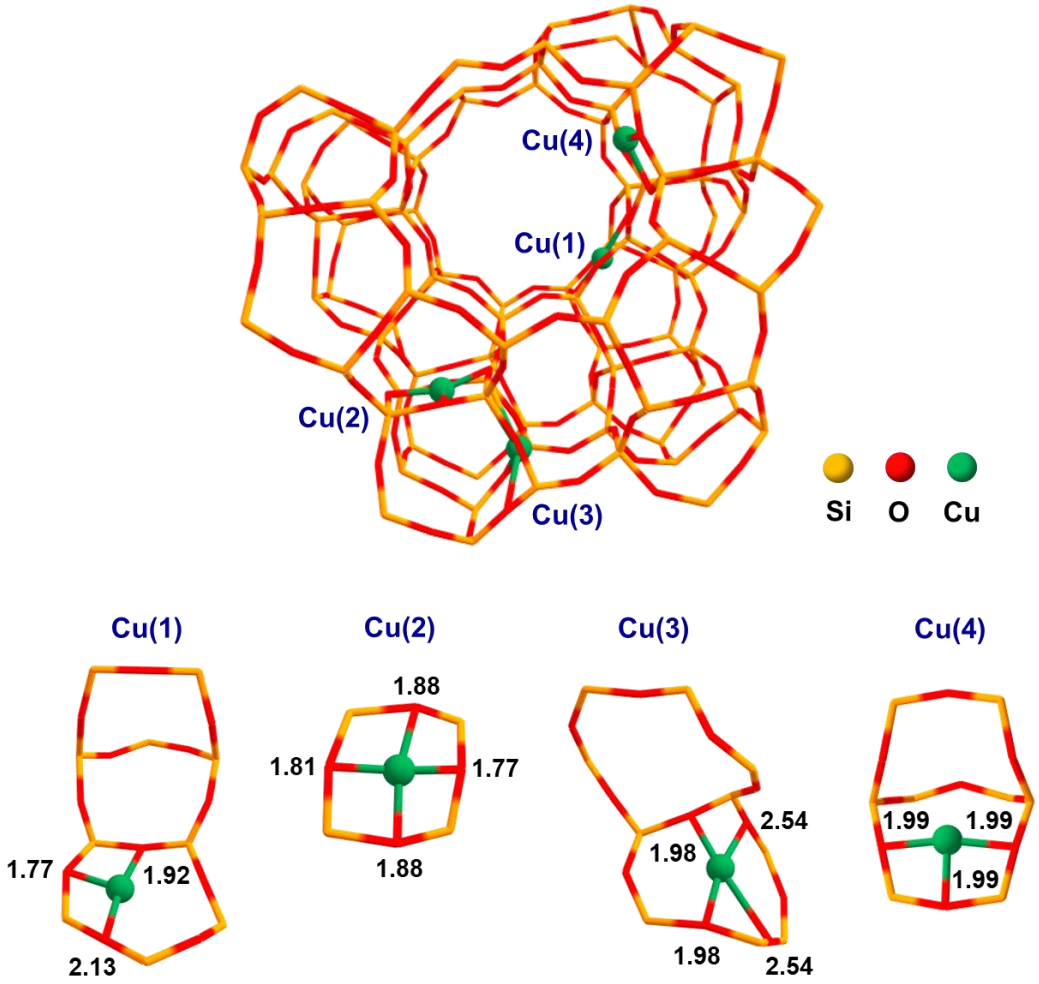

Figure S5. Positions of Cu^{2+} ions within Cu^{2+}/H-ZSM-5 zeolite identified using the Rietveld refinement of the XRD data (Figure S4, Table S3). The nearest Cu–O distances (Å) are given in black. Note that the positions of Al atoms compensating for the Cu^{2+} charge could not be identified with Rietveld analysis due to the low sensitivity of X-rays to differences in one electron between Si and Al.

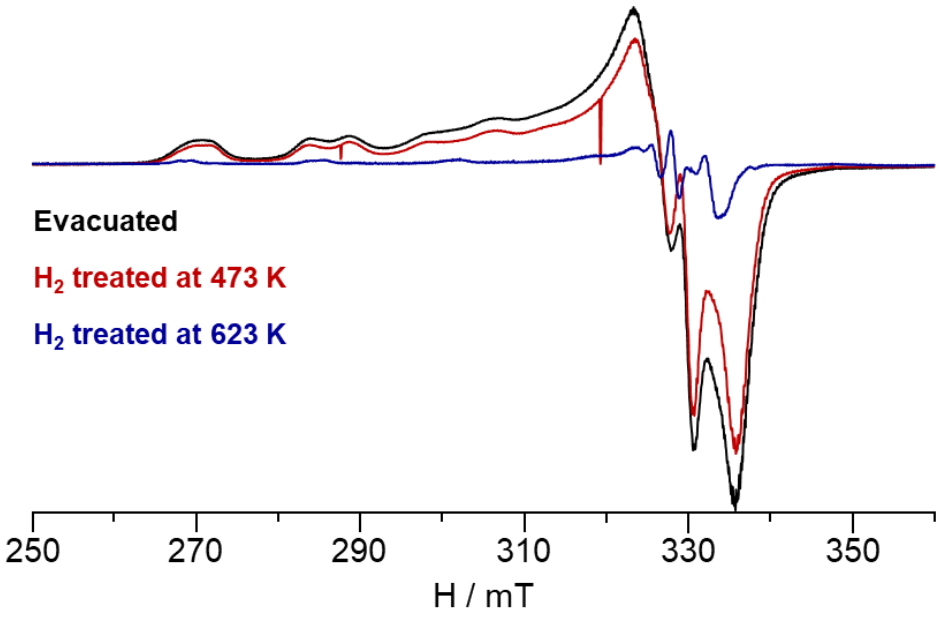

Figure S6. EPR spectra of Cu/H-ZSM-5 samples: evacuated at 673 K for 18 h (black line), H_2-treated at 473 K (red line), and H_2-treated at 623 K (dark blue line).

Reductive treatment was performed in the following way. First, ion-exchanged Cu/H-ZSM-5 sample was evacuated upon heating to 673 K at 1.3 K min^{-1} rate and keeping at 673 K for 18 h (residual pressure < 10^{-3} Pa). Then, the sample was exposed to 200 mbar static pressure of H_2 for 1 h at 473 K or 623 K, followed by evacuation at the same temperature for 1 h.

The reduction of Cu^{2+} ions under different conditions was monitored by EPR spectroscopy. As can be seen from Figure S6, after H_2-treatment at 473 K, the concentration of Cu^{2+} ions decreases only slightly (integrated intensity is about 1.4 times lower compared to the initial evacuated Cu/H-ZSM-5 sample). On the contrary, after H_2-treatment at 623 K, the concentration of Cu^{2+} ions decreases significantly (integrated intensity is about 18 times lower compared to the initial evacuated Cu/H-ZSM-5 sample). Therefore, the treatment at 623 K provides almost full reduction of Cu^{2+} sites in the sample. To examine the state of copper in the reduced sample (Cu^{+} or Cu^{0}), XPS method was used (Figure S7).

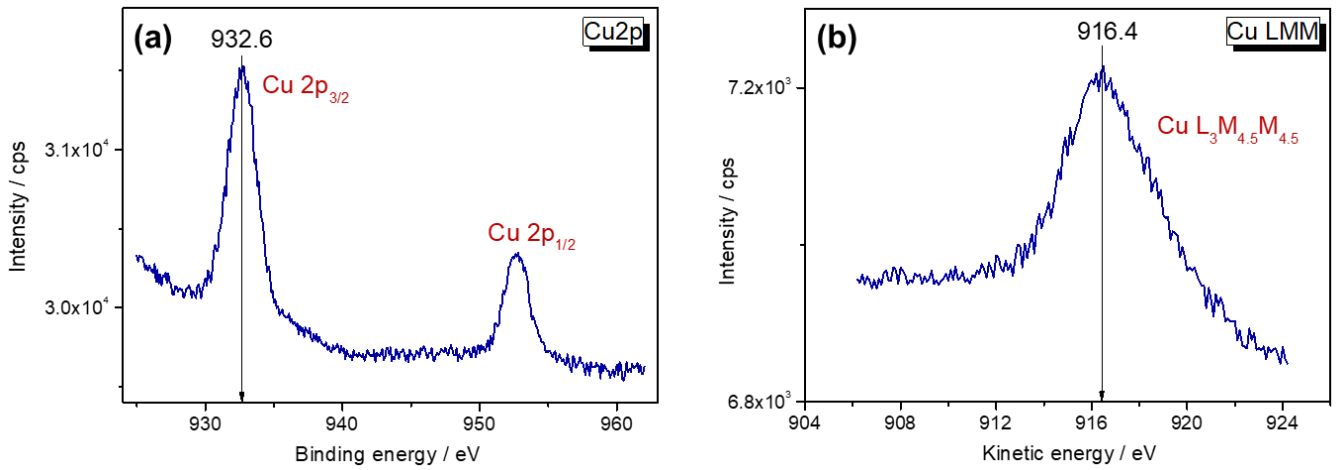

Figure S7. Cu 2p (a) and Cu LMM (b) XPS spectra of Cu/H-ZSM-5 sample treated with H_2 at 623 K (referred to as Cu^+/H-ZSM-5).

The observed Cu $2p_{3/2}$ core-level XPS spectrum is well described by a single line, suggesting only one type of copper chemical state. The modified Auger parameter, which is the sum of Cu $2p_{3/2}$ binding energy value and the kinetic energy of $L_3M_{4.5}M_{4.5}$ Auger peak, amounts to 1849.0 eV, which corresponds to Cu^+ state.[13-15] Therefore, according to XPS data, after H_2 treatment of Cu/H-ZSM-5 at 623 K, Cu^{2+} species are reduced to Cu^+ species rather than to Cu^0 species.

Note that ^{1}H MAS NMR data presented in Figure S2 are also in favor of Cu^{2+} species reduction to Cu^+ state, since not all Si–O(H)–Al groups are regenerated, and their concentration corresponds to the copper content in the sample considering the stabilization of Cu^+ ions at Si–O^-–Al positions.

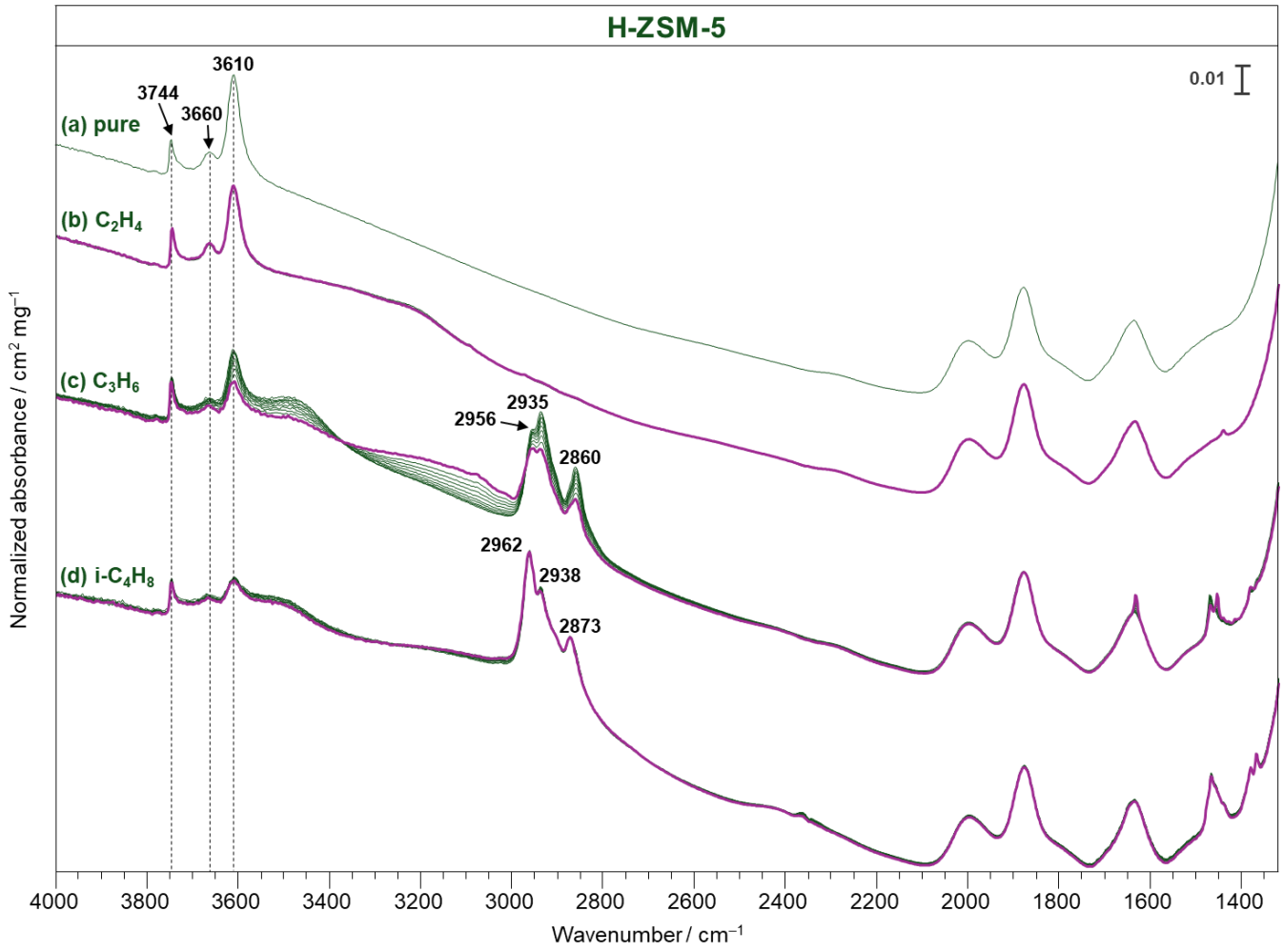

Figure S8. FTIR spectra of pure H-ZSM-5 sample (a) and alkenes adsorbed on H-ZSM-5: ethene (b), propene (c), and isobutene (d). Alkenes were adsorbed on the zeolite sample at 77 K, followed by transferring the cell with the sample to the spectrophotometer and spectrum recording at 296 K. In (b)–(d), multiple spectra were recorded successively, with 10 scans acquired for each spectrum to monitor by FTIR spectroscopy if any noticeable transformations occurred at 296 K within a timespan of ~ 3 minutes. The first spectrum in each series is shown by a violet thick line.

It should be noted that the spectrum of pure H-ZSM-5 zeolite (Figure S8a) does not contain the bands from any organic impurities in the C–H stretching region (3000–2800 cm^{-1}).

In the OH-stretching region, the bands at 3744, 3660, and 3610 cm^{-1} are observed which belong to Si–OH, Al–OH, and Si–O(H)–Al groups of the zeolite, respectively.[16] Upon alkene adsorption on Si–O(H)–Al groups, the band at 3610 cm^{-1} is broadened and redshifted due to the perturbation of O–H stretching vibration and alkene–H^+ complex formation. In the C–H stretching region, overlapping bands are observed for propene (2860, 2935, and 2956 cm^{-1}) and isobutene (around 2873, 2938, and 2962 cm^{-1}) which are related to the vibrations of the $–CH_2–$ and $–CH_3$ groups of oligomer species.[17-19]

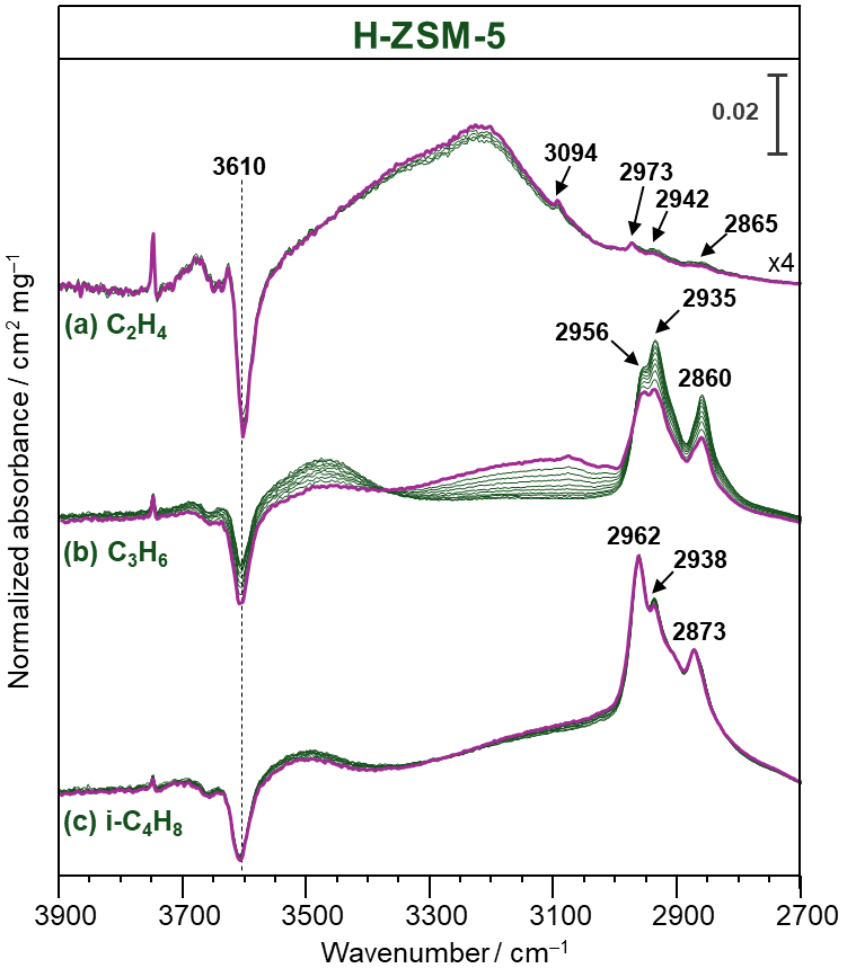

Figure S9. FTIR spectra of ethene (a), propene (b), and isobutene (c) adsorbed on H-ZSM-5 in the 3900–2700 cm^{-1} region. Alkenes were adsorbed on the zeolite sample at 77 K, followed by transferring the cell with the sample to the spectrophotometer and multiple spectrum subsequent recording at 296 K. The first spectrum in each series is shown by a violet thick line. The spectrum of pure H-ZSM-5 was subtracted from the spectra with adsorbed alkenes (for the original spectra, see Figure S8).

For ethene, oligomerization is slower, and the bands from ethene (3094 cm^{-1}, $\nu_a(=CH_2)$, 2973 cm^{-1}, $\nu_s(=CH_2)$) and from oligomeric species (around 2942 and 2865 cm^{-1}, $\nu(–CH_2–)$) are detected. Overlapping bands are observed for propene (2860, 2935, and 2956 cm^{-1}) and isobutene (around

2873, 2938, and 2962 cm^{-1}) which are related to the vibrations of the $–CH_2–$ and $–CH_3$ groups of oligomer species.[17-19] The band at 3610 cm^{-1} belongs to Si–O(H)–Al group stretching vibration. It is seen as a negative band in the subtracted spectra due to alkene interaction with Si–O(H)–Al groups leading to the ν(OH) vibration perturbation (band shift and broadening).[16]

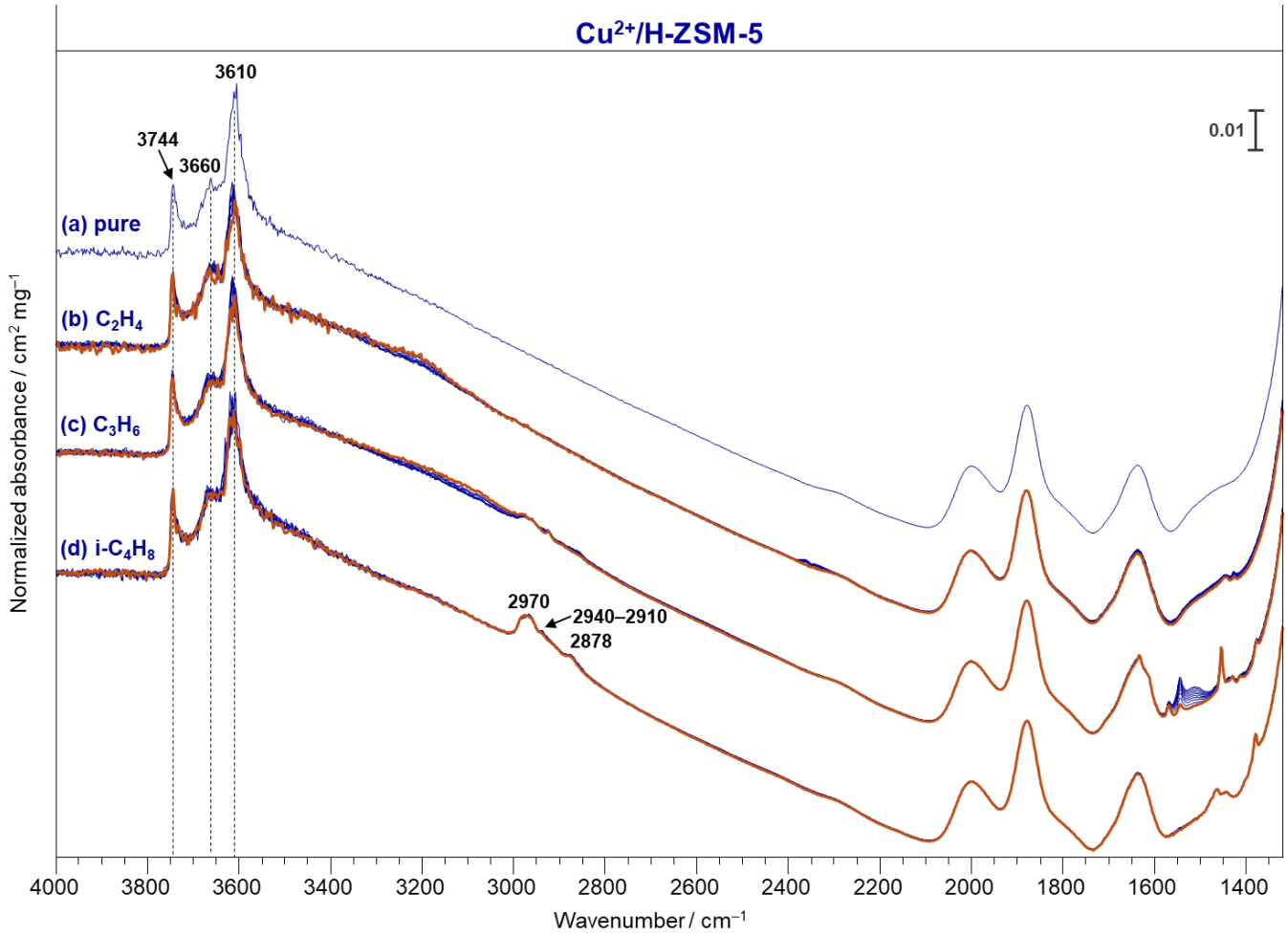

Figure S10. FTIR spectra of pure Cu^{2+}/H-ZSM-5 sample (a) and alkenes adsorbed on Cu^{2+}/H-ZSM-5: ethene (b), propene (c), and isobutene (d). Alkenes were adsorbed on the zeolite sample at 77 K, followed by transferring the cell with the sample to the spectrophotometer and spectrum recording at 296 K. In (b)–(d), multiple spectra were recorded successively, with 10 scans acquired for each spectrum to monitor by FTIR spectroscopy if any noticeable transformations occurred at 296 K within a timespan of ~ 3 minutes. The first spectrum in each series is shown by a dark-orange thick line.

It should be noted that the spectrum of pure Cu^{2+}/H-ZSM-5 zeolite (Figure S10a) does not contain the bands from any organic impurities in the C–H stretching region (3000–2800 cm^{-1}).

In the OH-stretching region, the bands at 3744, 3660, and 3610 cm^{-1} are observed which belong to Si–OH, Al–OH, and Si–O(H)–Al groups of the zeolite, respectively.[16] Weak overlapping bands observed for isobutene (2878, 2940–2910, and 2970 cm^{-1}) are related to the vibrations of the $–CH_3$ groups (Figure S10d).[17, 18]

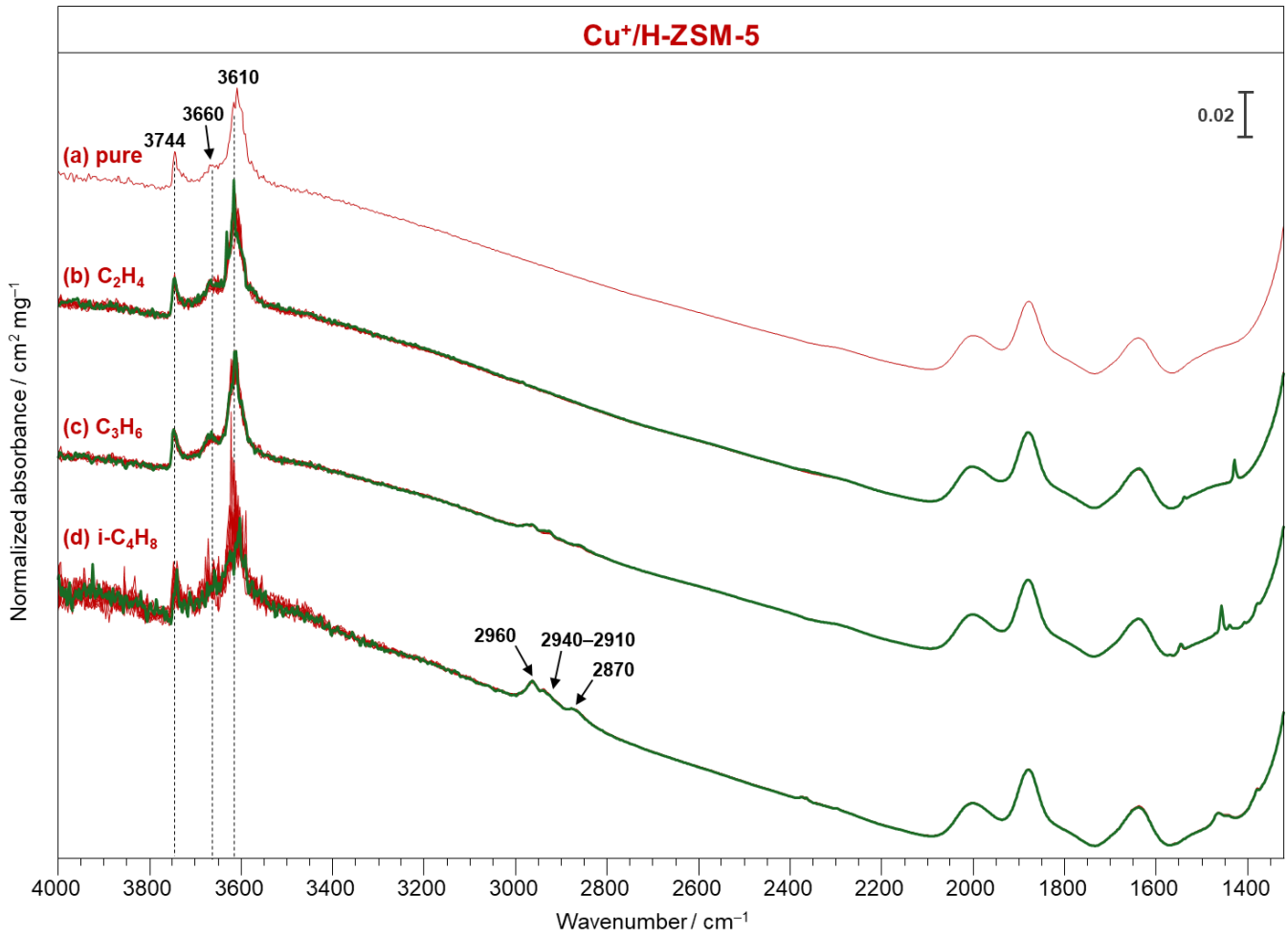

Figure S11. FTIR spectra of pure Cu^+/H-ZSM-5 sample (a) and alkenes adsorbed on Cu^+/H-ZSM-5: ethene (b), propene (c), and isobutene (d). Alkenes were adsorbed on the zeolite sample at 77 K, followed by transferring the cell with the sample to the spectrophotometer and spectrum recording at 296 K. In (b)–(d), multiple spectra were recorded successively, with 10 scans acquired for each spectrum to monitor by FTIR spectroscopy if any noticeable transformations occurred at 296 K within a timespan of ~ 3 minutes. The first spectrum in each series is shown by a dark-green thick line.

It should be noted that the spectrum of pure Cu^+/H-ZSM-5 zeolite (Figure S11a) does not contain the bands from any organic impurities in the C–H stretching region (3000–2800 cm^{-1}).

In the OH-stretching region, the bands at 3744, 3660, and 3610 cm^{-1} are observed which belong to Si–OH, Al–OH, and Si–O(H)–Al groups of the zeolite, respectively.[16] Weak overlapping bands observed for isobutene (2870, 2940–2910, and 2960cm^{-1}) are related to the vibrations of the $–CH_3$ groups (Figure S11d).[17, 18]

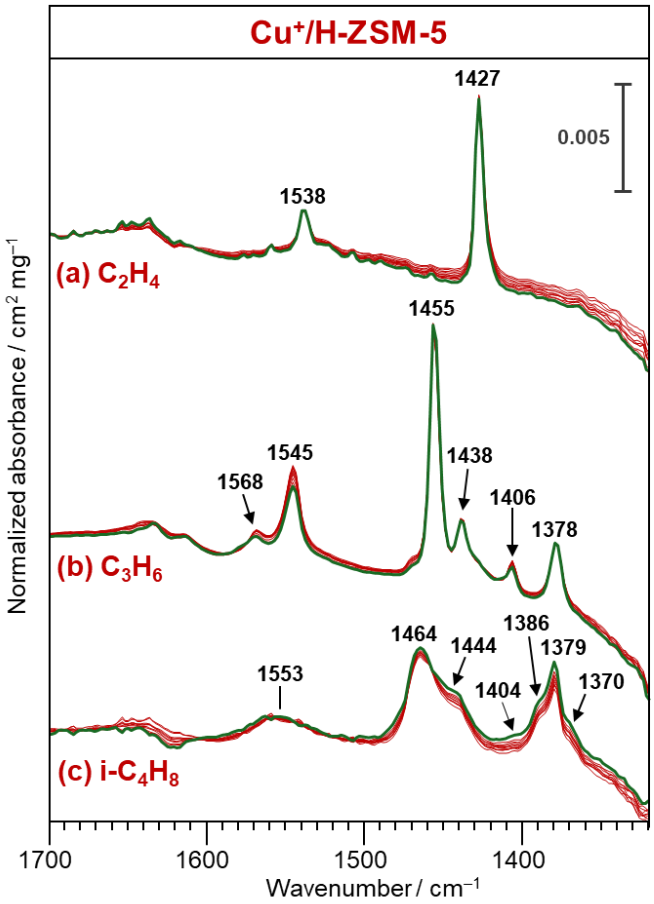

Figure S12. FTIR spectra of ethene (a), propene (b), and isobutene (c) adsorbed on Cu^+/H-ZSM-5 in the region of 1700–1300 cm^{-1}. Alkenes were adsorbed on the zeolite sample at 77 K, followed by transferring the cell with the sample to the spectrophotometer and multiple spectrum subsequent recording at 296 K. The first spectrum in each series is shown by a dark-green thick line. The spectrum of pure Cu^+/H-ZSM-5 was subtracted from the spectra with adsorbed alkenes (for the original spectra, see Figure S11).

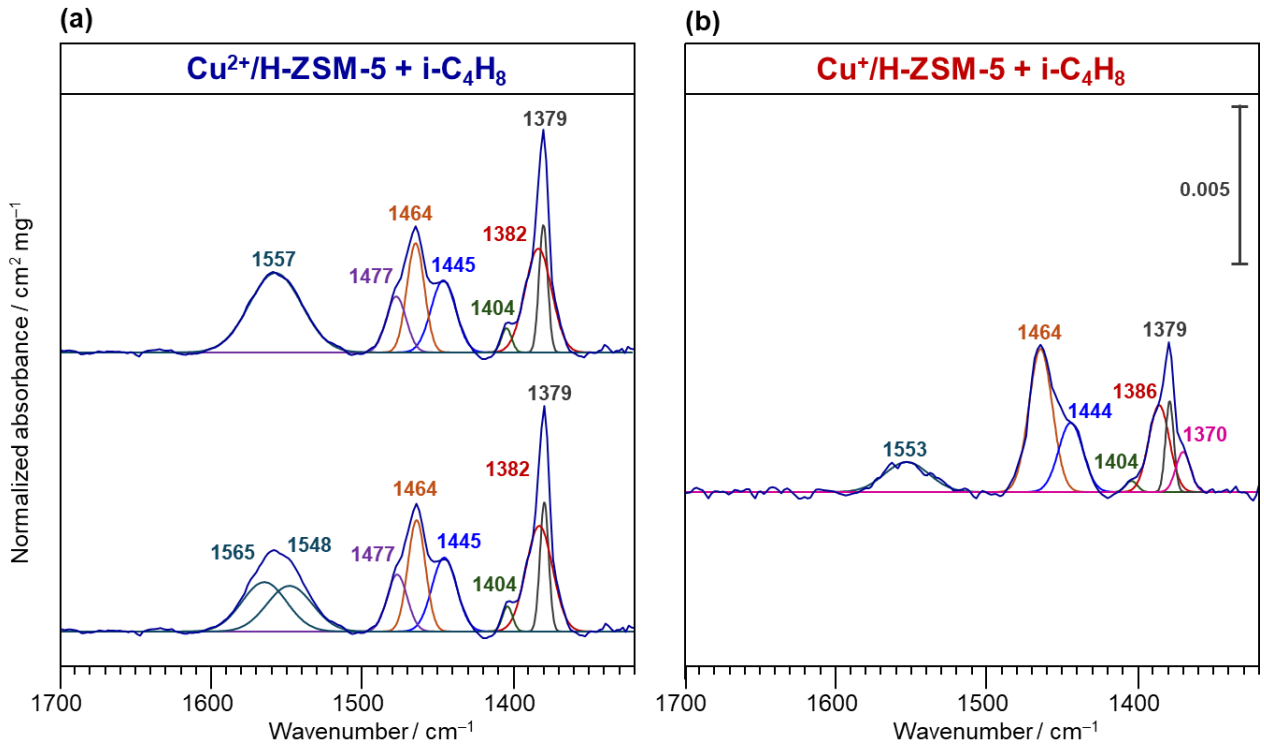

Figure S13. Possible deconvolution of baseline-corrected FTIR spectra of isobutene adsorbed on Cu^{2+}/H-ZSM-5 (a) and Cu^{+}/H-ZSM-5 (b) samples. For isobutene adsorbed on Cu^{2+}/H-ZSM-5, two possible deconvolutions are given which differ in the 1540–1560 cm^{-1} region. The spectra before baseline correction are presented in Figure 3e for Cu^{2+}/H-ZSM-5 and Figure 3f for Cu^{+}/H-ZSM-5. The assignment of the bands is given in Table 1.

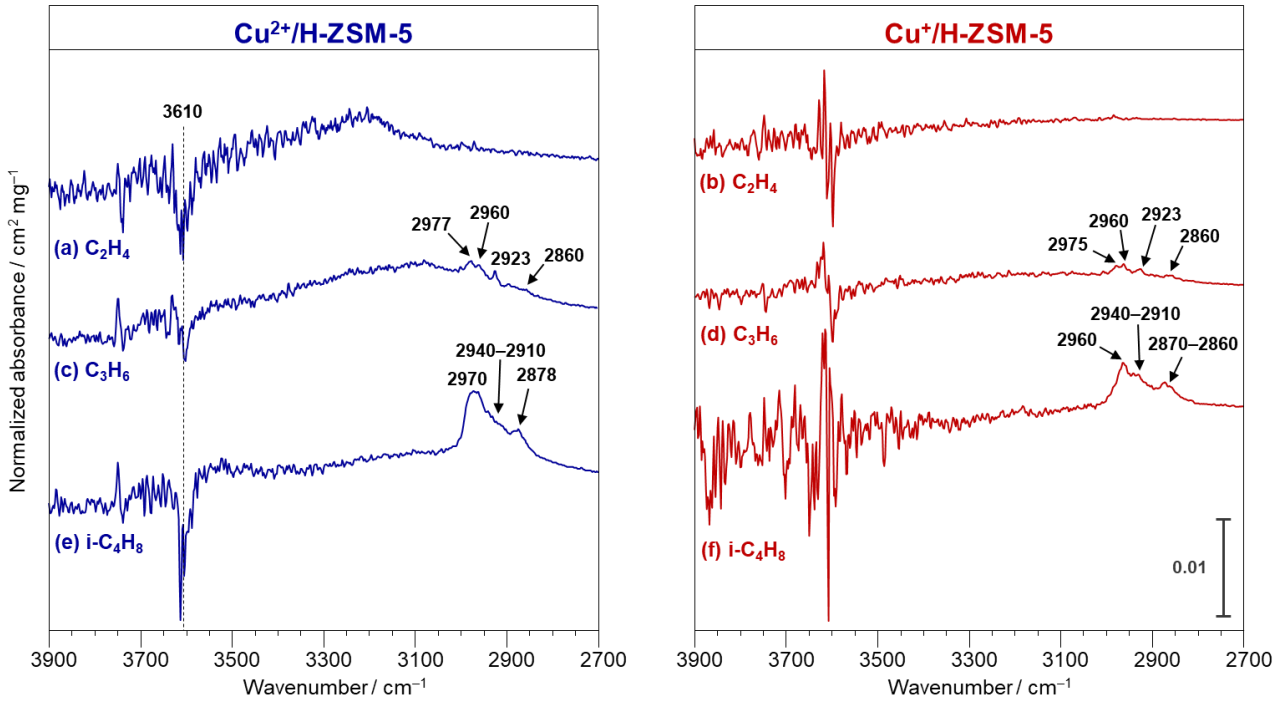

Figure S14. FTIR spectra of ethene (a, b), propene (c, d), and isobutene (e, f) adsorbed on Cu^{2+}/H-ZSM-5 (a, c, e) and Cu^{+}/H-ZSM-5 (b, d, f) samples in the 3900–2700 cm^{-1} region. Alkenes were adsorbed on the zeolite sample at 77 K, followed by transferring the cell with the sample to the spectrophotometer and spectrum recording at 296 K. The spectrum of pure zeolite sample (Cu^{2+}/H-ZSM-5 or Cu^{+}/H-ZSM-5) was subtracted from the spectra with adsorbed alkenes (for the original spectra, see Figures S10, S11).

Since only ten scans were accumulated for one spectrum, the spectra are of rather low intensity and not very informative for detailed analysis. Weak overlapping bands observed for propene (2860, 2923, 2960, and 2975–2977 cm^{-1}) and isobutene (2860–2870, 2940–2910, and 2960–2970 cm^{-1}) are related to the vibrations of the $–CH_3$ groups (Figure S14c,d,e,f).[17, 18] The band at 3610 cm^{-1} belongs to Si–O(H)–Al group stretching vibration. It is seen as a low-intensity negative band in the subtracted spectra, presumably due to alkene interaction with Si–O(H)–Al groups leading to the ν(OH) vibration perturbation (band shift and broadening).[16]

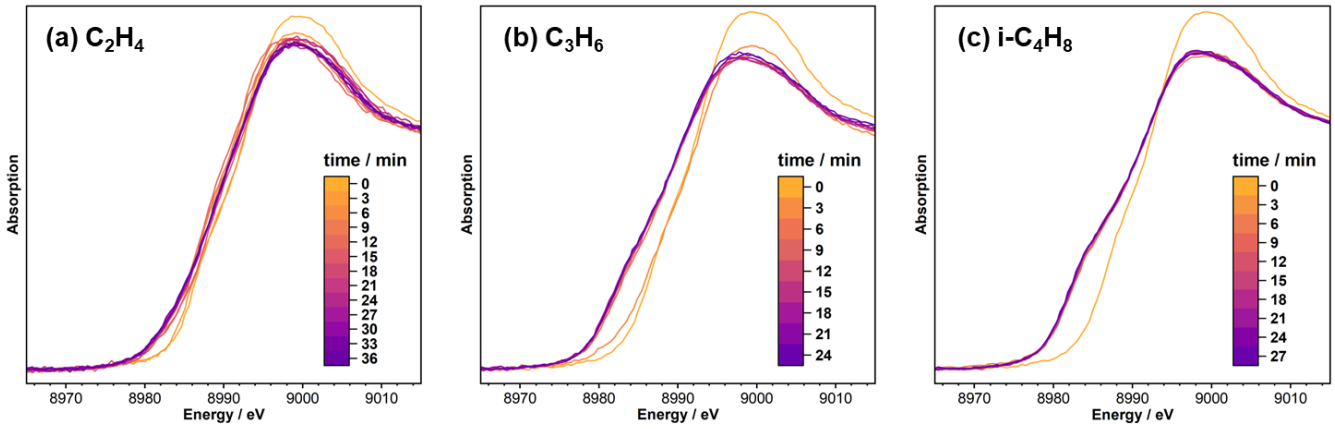

Figure S15. Copper K-edge XANES spectra for Cu^{2+}/H-ZSM-5 sample after the interaction with alkenes: ethene (a), propene (b), and isobutene (c). First, the Cu K-edge XANES spectrum of Cu^{2+}/H-ZSM-5 sample was measured (0 min). Then, the sample was exposed to alkene (C_2H_4, C_3H_6, or iso-C_4H_8) flow at 296 K, following Cu K-edge XANES spectrum recording to monitor the possible changes with time.

Table S1. Parameters of the Signals Used in Deconvolution of the ^{27}Al MAS NMR spectra of H-ZSM-5 and Cu/H-ZSM-5 samples (Figure S1)

Isotropic chemical shift (δ) / ppm	Quadrupole coupling constant (C_Q) / MHz	Asymmetry parameter (η)
H-ZSM-5		
57.8	2.38	0.52
59.6	3.31	0.52
56.1	5.38	0.44
2.6	3.05	0.63
18.6	6.03	0.75
Cu/H-ZSM-5		
56.92	2.34	0.54
59.28	3.24	0.52
67.53	5.73	0.64
2.67	3.00	0.29
28.19	7.23	0.08

Table S2. Lattice Parameters and Coherent Scattering Region Sizes Obtained from Rietveld Refinement Analysis of Cu^{2+}/H-ZSM-5 X-Ray Diffraction Pattern (Figure S3); Estimated Standard Deviations are Given in Parentheses

Phase (space group)	**Lattice parameter / Å**	**Coherent scattering region / nm**
Cu^{2+}/H-ZSM5 (*Pnma*)	*a* = 20.127 (0.001) *b* = 19.938 (0.001) *c* = 13.424 (0.001)	340 (20)
SiO_2 (Cristobalite, $P4_12_12$)	*a* = 4.89 (0.04) *c* = 7.20 (0.07)	2 (1)

Table S3 Rietveld Refinement Parameters for the Cu^{2+}/H-ZSM-5 Phase (Figure S3); Estimated Standard Deviations in the Last Character are Given in Parentheses

Atom	Coordinates (x, y, z)	Isotropic displacement factor U_{iso} / Å^2	Occupancy fraction
T(1)	0.423(4), 0.058(4), -0.339(5)	0.05(3)	1
T(2)	0.304(4), 0.031(4), -0.180(4)	0.04(3)	1
T(3)	0.274(4), 0.059(4), 0.024(4)	0.03(3)	1
T(4)	0.116(4), 0.063(4), 0.038(4)	0.03(3)	1
T(5)	0.073(4), 0.027(4), -0.179(4)	0.01(2)	1
T(6)	0.190(4), 0.059(4), -0.325(5)	0.03(1)	1
T(7)	0.426(4), -0.172(4), -0.332(5)	0.03(1)	1
T(8)	0.308(4), -0.131(4), -0.187(4)	0.03(1)	1
T(9)	0.278(4), -0.169(4), 0.030(4)	0.03(1)	1
T(10)	0.121(4), -0.175(4), 0.028(4)	0.02(3)	1
T(11)	0.068(4), -0.128(4), -0.190(4)	0.02(2)	1
T(12)	0.186(4), -0.172(4), -0.313(5)	0.04(2)	1
O(1)	0.371(8), 0.050(9), -0.241(9)	0.06(4)	1
O(2)	0.310(8), 0.071(6), -0.08(1)	0.06(4)	1
O(3)	0.191(8), 0.052(8), 0.032(8)	0.05(4)	1
O(4)	0.099(5), 0.058(8), -0.061(9)	0.05(2)	1
O(5)	0.121(8), 0.065(8), -0.265(9)	0.05(2)	1
O(6)	0.247(8), 0.045(9), -0.256(9)	0.05(2)	1
O(7)	0.382(8), -0.155(8), -0.225(9)	0.06(6)	1
O(8)	0.306(8), -0.151(6), -0.073(8)	0.03(4)	1
O(9)	0.186(8), -0.157(6), 0.036(8)	0.04(2)	1
O(10)	0.086(8), -0.158(8), -0.089(9)	0.04(2)	1

O(11)	0.122(8), -0.148(8), -0.243(8)	0.04(4)	1
O(12)	0.242(8), -0.143(8), -0.255(9)	0.04(4)	1
O(13)	0.309(9), -0.045(8), -0.169(8)	0.09(6)	1
O(14)	0.078(6), -0.054(8), -0.182(8)	0.04(2)	1
O(15)	0.414(6), 0.126(6), -0.40(1)	0.04(2)	1
O(16)	0.413(6), 0.007(8), -0.433(9)	0.03(4)	1
O(17)	0.099(8), 0.133(8), 0.08(1)	0.05(2)	1
O(18)	0.185(6), 0.132(6), -0.369(9)	0.04(4)	1
O(19)	0.290(8), 0.003(8), 0.106(8)	0.04(4)	1
O(20)	0.302(8), 0.129(7), 0.072(8)	0.04(4)	1
O(21)	0.507(8), 0.049(8), -0.293(8)	0.03(4)	1
O(22)	0.500(9), -0.157(8), -0.289(8)	0.05(6)	1
O(23)	0.42(1), -0.25, -0.36(1)	0.06(6)	1
O(24)	0.20(1), -0.25, -0.34(1)	0.06(6)	1
O(25)	0.29(1), -0.25, 0.06(2)	0.09(8)	1
O(26)	0.11(1), -0.25, 0.07(2)	0.04(2)	1
O(27) – water	-0.23(1), 0.25, 0.08(2)	0.05(5)	0.6(1)
O(28) – water	0.55(2), 0.25, -0.21(2)	0.05(5)	0.5(2)
Cu(1)	0.36(1), 0.02(1), 0.22(2)	0.06(4)	0.09(3)
Cu(2)	0.29(1), 0.25, 0.54(5)	0.08(7)	0.06(2)
Cu(3)	0.41(3), 0.25, 0.36(4)	0.06(7)	0.07(2)
Cu(4)	0.19(8), 0.25, 0.41(3)	0.05(8)	0.03(1)

REFERENCES

1. G. Engelhardt and D. Michel, *High-Resolution Solid-State NMR of Silicates and Zeolites*, John Wiley & Sons, Chichester, 1987.
2. D. Massiot, F. Fayon, M. Capron, I. King, S. Le Calvé, B. Alonso, J. O. Durand, B. Bujoli, Z. Gan and G. Hoatson, *Magn. Reson. Chem.*, 2002, **40**, 70–76.
3. A. A. Gabrienko, I. G. Danilova, S. S. Arzumanov, L. V. Pirutko, D. Freude and A. G. Stepanov, *J. Phys. Chem. C*, 2018, **122**, 25386–25395.
4. D. H. Olson, W. O. Haag and R. M. Lago, *J. Catal.*, 1980, **61**, 390–396.
5. E. L. Wu, S. L. Lawton, D. H. Olson, A. C. Rohrman and G. T. Kokotailo, *J. Phys. Chem.*, 1979, **83**, 2777–2781.
6. H. van Koningsveld, H. van Bekkum and J. C. Jansen, *Acta Crystallographica Section B*, 1987, **43**, 127–132.
7. B. Toby, *Journal of Applied Crystallography*, 2024, **57**, 175–180.
8. B. F. Mentzen and G. Bergeret, *J. Phys. Chem. C*, 2007, **111**, 12512–12516.
9. M. H. Groothaert, K. Pierloot, A. Delabie and R. A. Schoonheydt, *Phys. Chem. Chem. Phys.*, 2003, **5**, 2135–2144.
10. J. Dědeček, D. Kaucký and B. Wichterlová, *Microporous Mesoporous Mater.*, 2000, **35–36**, 483–494.
11. A. A. Gabrienko, E. S. Kvasova, D. I. Kolokolov, D. E. Gorbunov, A. S. Nizovtsev, Z. N. Lashchinskaya and A. G. Stepanov, *Inorg. Chem.*, 2024, **63**, 5083–5097.
12. A. A. Shubin, G. M. Zhidomirov, V. B. Kazansky and R. A. Van Santen, *Cat. Lett.*, 2003, **90**, 137–142.
13. M. C. Biesinger, *Surface and Interface Analysis*, 2017, **49**, 1325–1334.
14. I. Khalakhan, M. Vorokhta, X. Xie, L. Piliai and I. Matolínová, *J. Electron Spectrosc.*, 2021, **246**, 147027.
15. J. P. Espinós, J. Morales, A. Barranco, A. Caballero, J. P. Holgado and A. R. González-Elipe, *J. Phys. Chem. B*, 2002, **106**, 6921–6929.
16. G. Spoto, S. Bordiga, G. Ricchiardi, D. Scarano, A. Zecchina and E. Borello, *J. Chem. Soc. Faraday T.*, 1994, **90**, 2827–2835.
17. B. Silvi, P. Labarbe and J. P. Perchard, *Spectrochim. Acta A-M*, 1973, **29**, 263–276.
18. G. Busca, G. Ramis and V. Lorenzelli, *J. Chem. Soc. Farad. T 1*, 1989, **85**, 137–146.
19. M. Trombetta, G. Busca, S. Rossini, V. Piccoli and U. Cornaro, *J. Catal.*, 1997, **168**, 349−363.